The International Journal of Advanced Manufacturing Technology (2019) 101:1349–1356
https://doi.org/10.1007/s00170-018-2927-4

ORIGINAL ARTICLE

Effect of in-process active cooling on forming quality and efficiency of tandem GMAW–based additive manufacturing

Junbiao Shi [1,2] · Fang Li [1,2] · Shujun Chen [1,2] · Yun Zhao [1,2] · Hongyu Tian [1,2]

Received: 10 May 2018 / Accepted: 23 October 2018 / Published online: 19 November 2018
© Springer-Verlag London Ltd., part of Springer Nature 2018

Abstract

Wire arc additive manufacturing (WAAM), utilizing welding arc to melt metal wire into shaped parts, has become a promising manufacturing technology recently. Tandem GMAW–based WAAM (TG-WAAM), in which two wires are fed into the molten pool simultaneously, has the potential to double the efficiency of traditional WAAM. However, the high wire-feed speed is accompanied with high heat input that is likely to cause molten pool overflowing, especially at upper layers because of decreased heat dissipation and increased heat accumulation. An in-process active cooling technology based on thermoelectric cooling is introduced into TG-WAAM in this research. Its effect on forming quality and efficiency of TG-WAAM is investigated experimentally. The results show that the additional cooling well compensates for the excessive heat input into the molten pool, which enables not only increased maximum wire-feed speed (9–15%) but also reduced inter-layer dwell time (42–54%), while maintaining the desired forming quality. The overall efficiency is improved by more than 0.97 times in the case study. This research provides a feasible scheme to solve the conflict between forming quality and efficiency during WAAM.

Keywords Wire arc additive manufacturing · Tandem GMAW · Active cooling · Forming quality · Efficiency

1 Introduction

Additive manufacturing (AM), which fabricates components in a layer-by-layer pattern, has become a promising manufacturing technology with huge growth potential in the past 30 years [1]. It offers much higher geometrical flexibility and greater potential of time and cost savings compared with conventional manufacturing technologies. Recently, AM for functional metal components, instead of plastic prototypes, has become a hot topic in order to meet the demanding requirements of the aerospace industries. For any metallic AM technology, the basic idea is to utilize a high energy source to melt metal material into shaped parts [2]. Laser and electron beam–based AM processes are commonly used [3]. However, their high cost and low efficiency (typically 0.12 kg/h for Ti–6Al–4V) greatly restrict their application in fabricating large metal components [4, 5].

In contrast, wire arc additive manufacturing (WAAM), utilizing welding arc to melt metal wire into shaped parts, well overcomes the obstacle above [6]. The maximum deposition rate can reach up to 2.6 kg/h for Ti–6Al–4V (much higher than SLM and EBM) and the cost of metal wire is about 1/10 of metal powder (much lower than SLM and EBM) [4, 7]. These characteristics make WAAM a good option to fabricate large metal components among various AM technologies [8]. For example, Cranfield University applied WAAM to fabricate a 1.2-m-long spar part for an airplane wing and Beijing University of Technology applied it to fabricate an integrally stiffened panel [9–11]. Different WAAM processes have been developed to meet different geometrical requirements, including GMAW-based, GTAW-based, and PAW-based processes. For example, CMT, a modified GMAW, is suitable to produce thin-walled structures, while PAW is suitable to produce wall structures of large width [12].

Efficiency is crucial for WAAM when large metal components are concerned. In order to obtain higher efficiency, the wire-feed speed (WFS) should be increased to deposit more material per unit time and so is the welding current to increase

✉ Fang Li
lif@bjut.edu.cn

[1] College of Mechanical Engineering and Applied Electronics Technology, Beijing University of Technology, Beijing 100124, China

[2] Engineering Research Center of Advanced Manufacturing Technology for Automotive Components-Ministry of Education, Beijing University of Technology, Beijing 100124, China

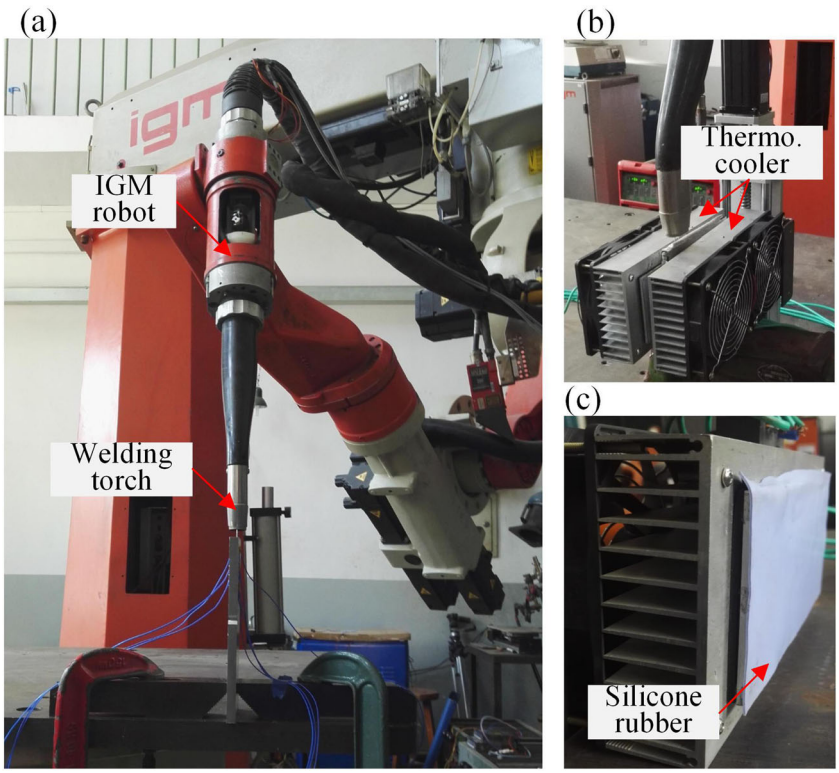

Fig. 1 **a** IGM Robot system for TG-WAAM. **b**, **c** Thermoelectric cooler

the melting energy. However, this will inevitably bring extra heat into the molten pool that is directly coupled with the heat for melting the metal wire [13]. Along with high heat input are reduced viscosity of the material, large arc force, and strong droplet impingement, which are likely to lead to molten pool overflowing, making it difficult to obtain the desired forming quality. As the deposition height increases, the heat dissipation condition will become worse and the heat accumulation will become more serious. This is because in this case the heat is dissipated not only to the substrate through conduction but also to the air through convection and radiation. However, the latter is less effective than the former [14]. These reasons add more difficulty to control the shape of the molten pool and ultimately the forming quality. Therefore, the forming quality and efficiency conflict each other during WAAM. It is challenging to achieve a high efficiency while maintaining the desired forming quality [15, 16].

An alternative way to increase the efficiency is to employ multiple wire processes, such as tandem GMAW and twin-wire GTAW. For tandem GMAW, two wires are fed from a single special torch simultaneously along with the direction of travel, whereas for twin-wire GTAW two wires are fed from two separate wire-feed systems [17]. They provide the possibility to double the efficiency of traditional single-wire WAAM. However, multiple wire processes require much higher heat input than single wire processes to increase the melting energy, which means that the molten pool shape and the forming quality are more difficult to control. Previous studies mainly focus on the application of multiple wire processes to the production of intermetallic and functionally graded materials, but few focus on how to realize the full potential of their high WFS [18].

During WAAM, the molten pool shape is affected by not only the heat input but also the heat dissipation. Though the heat input is high, it is still possible to well control the molten pool shape by enhancing the heat dissipation via additional cooling to compensate for the excessive heat input. This provides the possible to solve the conflict between forming quality and efficiency during WAAM [19]. Fayolle applied cryogenic liquid argon cooling to prevent heat accumulation during

Table 1 Experiment design

Group no.	Heat dissipation condition	WFS (m/min)	TS (cm/min)
I	At the lower layer without cooling	2, 3, 4, 5, 6, 7	20, 30, 40, 50, 60, 70, 80, 90, 100
II	At the upper layer without cooling	2, 3, 4, 5, 6, 7	20, 30, 40, 50, 60, 70, 80, 90, 100
III	At the upper layer with cooling	2, 3, 4, 5, 6, 7	20, 30, 40, 50, 60, 70, 80, 90, 100

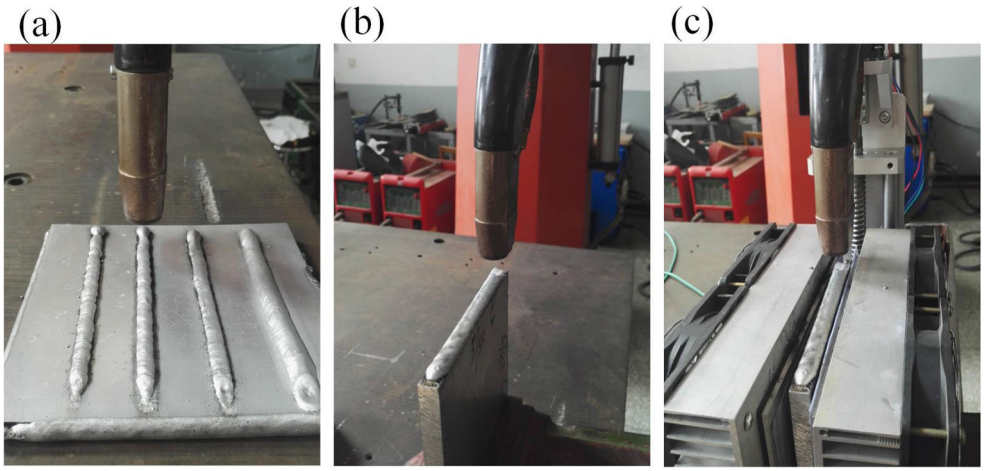

Fig. 2 **a** Deposition on a flat substrate. **b** Deposition on an existing wall without cooling. **c** Deposition on an existing wall with cooling

WAAM and the efficiency was proved to be tripled. Henckell presented that gas cooling improved the buildup condition that enabled a continuous manufacturing process without heat accumulation in the top layers [20, 21]. However, the air cooling setup should not be too close to the molten pool because the stability of the welding arc is likely to be disrupted. Therefore, it affects the molten pool mainly during the period after it is solidified that contributes to reducing the inter-layer dwell time, but has limited effect on the shape of the molten pool before it is solidified. To address this issue, this research introduces in-process active cooling into TG-WAAM based on the thermoelectric technology, which can be quite close to the molten pool. With the help of the strong heat conduction of the thermoelectric cooling technology, the low heat dissipation rate via convection and radiation is enhanced significantly. Therefore, it has significant effect on the molten pool both before and after it is solidified, thereby leading to both increased WFS and reduced inter-layer dwell time. The effect of in-process active cooling on the forming quality and efficiency of TG-WAAM is investigated in the rest of this paper.

2 Methodology

2.1 Experimental setup

Figure 1a shows the experimental setup to implement TG-WAAM. An IGM industrial robot is used to control the movement of the torch. Two separate wire-feed units along with two Fronius power supplies are used to control the two wires, which are fed through the same torch and are placed in-line with each other along the direction of the travel. The power supplies are operated under the pulse transfer mode. The substrate is high-strength aluminum alloy 2219 (6.3% Cu), which has wide application in the aerospace industry [22]. The wire electrode is aluminum alloy 2325 with similar chemical composition as 2219 and a 1.2-mm diameter.

Two thermoelectric coolers are employed for in-process active cooling, which are partly placed symmetrically towards the two sides of the wall structure, as shown in Fig. 1b. The basic function of a thermoelectric cooler is

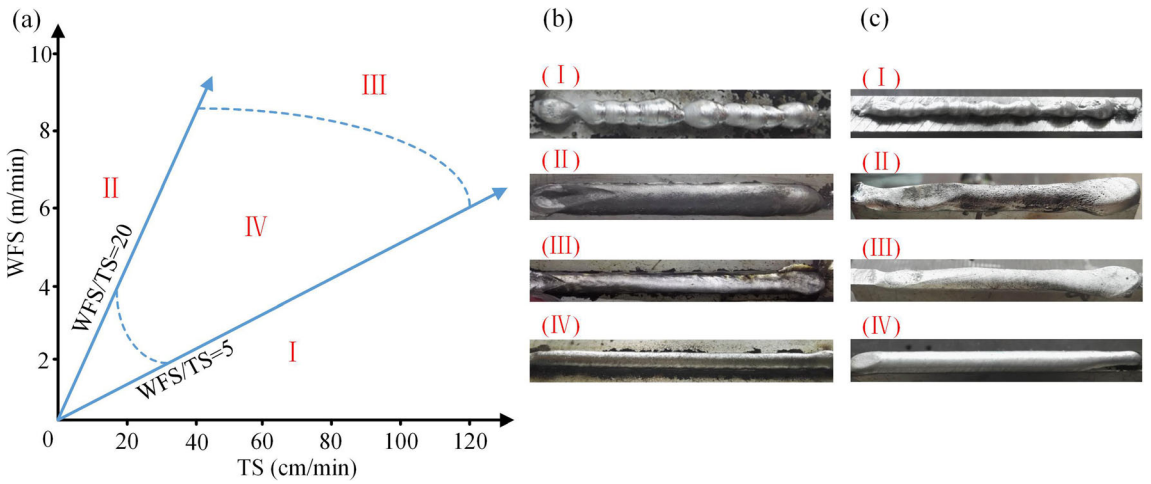

Fig. 3 **a** Process parameter area of various forming appearances: **b** forming appearances at the lower layer (group I); **c** forming appearances at the upper layer (group II)

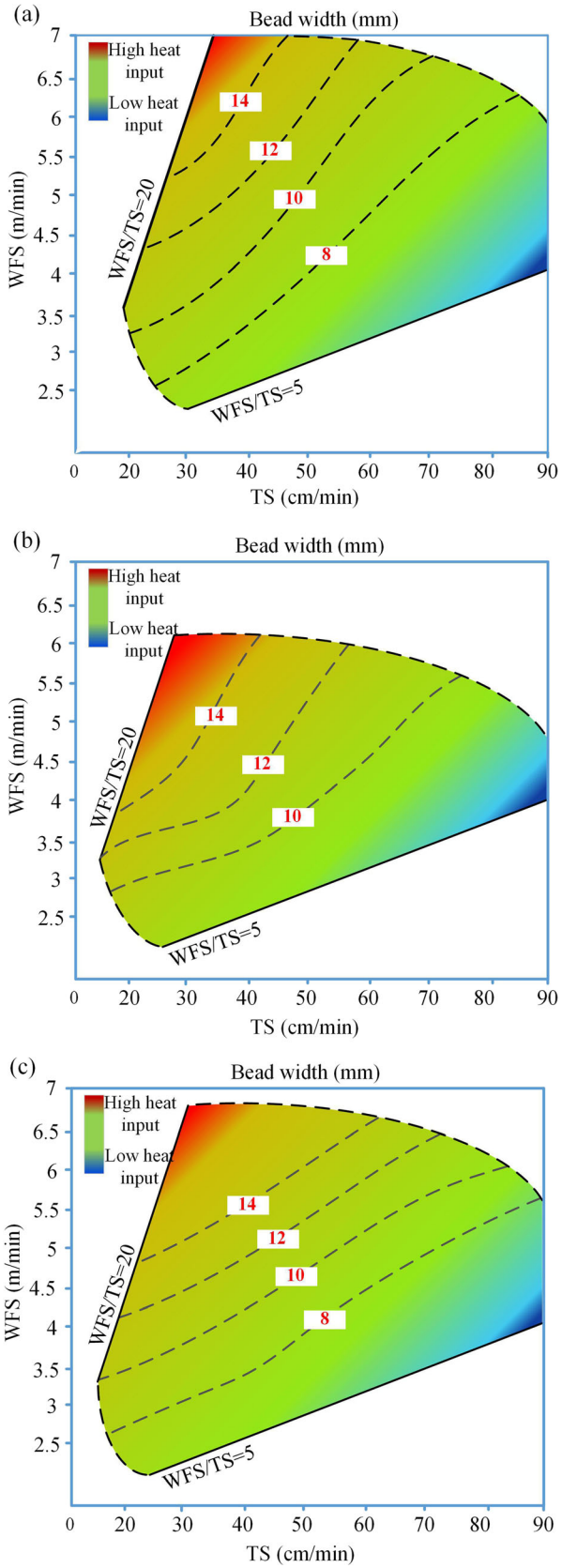

Fig. 4 Bead width contour **a** at the lower layer without cooling (group I), **b** at the upper layer without cooling (group II), and **c** at the upper layer with cooling (group III)

to transfer heat from the hot side to the cold side, consuming electrical energy. Then the excessive heat input into the molten pool can be transferred to the ambient environment quickly. Compared with gas or liquid cooling methods, the primary advantages of thermoelectric coolers include no leakage, flexible shape, long life, and controllable cooling rate [23]. For the thermoelectric cooler used in this study, its cooling power can be easily controlled through adjusting the DC voltage [24].

Preliminary experiments show that if the thermoelectric cooler does not contact well with the side of the wall, given that the wall surface is not flat due to the stair-stepping effect, the cooling effect is not obvious. To address this issue, a silicone rubber with high thermal conductivity is employed to guarantee good contact between the thermoelectric cooler and the wall. Its thickness is 2 mm, as shown in Fig. 1c. This cooling setup can also move in the Z direction as the deposition height increases, driven by a step motor.

2.2 Experimental design

Several experiments were conducted to explore the effect of different heat dissipation conditions (group I–group III) on forming quality and efficiency of TG-WAAM under various process parameters, as given in Table 1. Travel speed (TS) and wire-feed speed (WFS) were selected as the main influencing factors. WFS was varied from 2 to 7 m/min with an interval of 1 m/min and TS was varied from 20 to 100 cm/min with an interval of 10 cm/min. Different combination of WFS and TS generated different forming quality and efficiency.

The experiments were conducted on a flat substrate and an existing wall in group I and group II/III respectively to reflect the heat dissipation condition at different heights. The flat substrate in group I has dimensions of 150 mm (width) × 150 mm (length) × 6 mm (height) (see Fig. 2a) and the existing wall in group II and III has the same dimensions as the flat substrate (see Fig. 2b, c). From these experiments, we can analyze (1) the effect of deposition height on forming quality and efficiency of TG-WAAM by comparing group I and group II and (2) the effect of the additional cooling on forming quality and efficiency of TG-WAAM by comparing groups II and III.

In these experiments, the molten pool was detected through a high-speed camera MotionPro Y4S1. The bead geometry after the solidification of the molten pool, characterized by bead width and bead height, was measured through a laser displacement scanner. The thermal cycling was recorded through a thermocouple of type K, which was mounted at a depth of 5 mm from the upper surface.

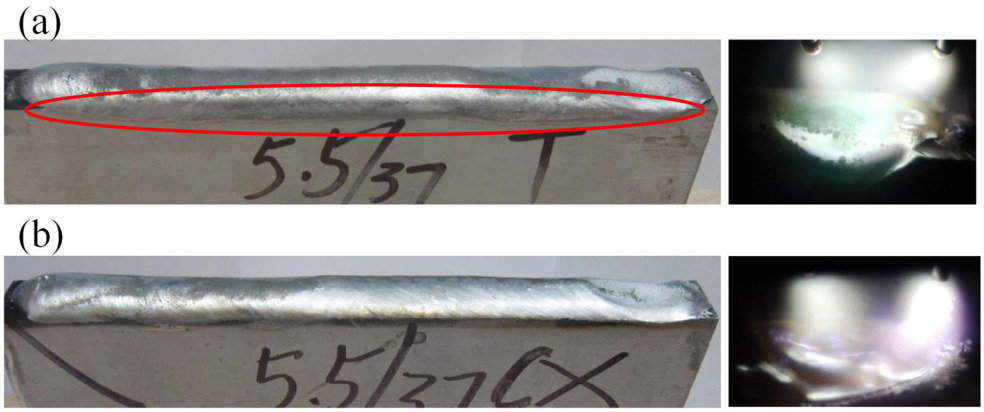

Fig. 5 Forming appearance and molten pool shape: **a** at the upper layer without cooling (group II) and **b** at the upper layer with cooling (group III)

3 Results and discussions

3.1 Comparison of forming appearance in the three cases

Based on the experimental results (according to Table 1), the relation between the forming appearance with the process parameters under different heat dissipation conditions was established, as shown in Fig. 3. The contour plot was also generated to represent graphically the relation between the bead width and the process parameters, as shown in Fig. 4. The process window, which reflects the feasible parameter ranges that allows good forming appearance, is confined to the area where WFS/TS is between 5 and 20 basically. For any of the three cases, the process parameter area can be divided into four regions, which differ in their heat input. As is known, the heat input per unit length increases with the increase of the welding current and the welding voltage, and the decrease of the TS. Because the control system is operated under the unified parameter regulation control mode, the welding current is an increasing function of the WFS. In region I with relatively small WFS and large TS, the heat input is quite small. The welding arc is not stable and the weld toe is incompletely melted. In region II with relatively large WFS and small TS, the heat input is large enough to spread the molten pool. However, the molten pool contains excessive heat that easily results in overflowing and wrinkles. In region III with relatively large WFS and large TS, the bead width and height is likely to change irregularly, even producing scallops and humps. This can be explained by the strong droplet impingement and the large arc force. In region IV, the forming appearance is quite excellent with no obvious defects and spatters and therefore is suitable for WAAM.

By comparing the process windows of group I and group II, it can be concluded that the process window obtained at the lower layer is larger than that obtained at the upper layer, as shown in Fig. 4a, b. At the high heat input region, the forming appearance is excellent at the lower layer as shown in the group I, but is poor at the upper layer as shown in the group II. This result indicates that the heat dissipation condition of the molten pool becomes worse with the increase of the deposition height. Besides, the constraint of the base for the molten pool is relatively weak at the upper layer. Therefore, the molten pool overflowing is more likely to occur when the heat input is high. In other regions, though both their forming appearances are satisfactory, their bead width contours differ a lot. The contour line at the upper layer is shifted towards to the lower-right direction compared with that at the lower layer, which implies that the bead tends to be wider under the process parameters. This is because at lower layers with relatively

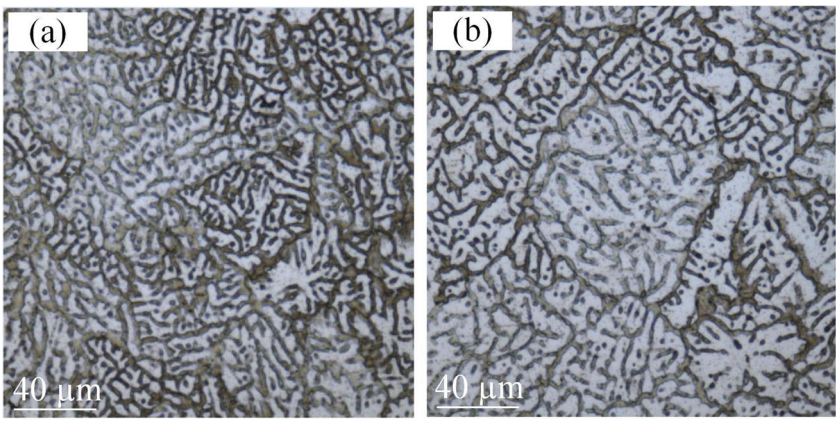

Fig. 6 Microstructures **a** with active cooling and **b** without active cooling

Table 2 Maximum wire-feed speed (deposition rate) versus bead width

	Bead width							
	8 mm		10 mm		12 mm		14 mm	
	DR (kg/h)	WFS (m/min)	DR (kg/h)	WFS (m/min)	DR (kg/h)	WFS (m/min)	DR (kg/h)	WFS (m/min)
Without cooling	1.83	5	1.97	5.5	2.12	5.8	2.03	6
With cooling	2.0	5.5	2.19	6.2	2.34	6.4	2.38	6.5
Improvement	10%	10%	11%	11%	9%	9%	15%	15%

fast heat dissipation, the molten pool solidifies quickly without enough time to form a wide bead and therefore the bead width tends to be smaller. At upper layers with relatively slow heat dissipation, the viscosity of the molten pool material is decreased and therefore the liquid metal tends to spread more easily, which leads to a larger bead width. The average increase of the bead width is 2 mm.

In group III with in-process active cooling, the process window is enlarged and the contour line is shifted towards to the upper-left direction compared with the situation in group II, as shown in Fig. 4c. The bead width decreases obviously (about 2 mm) with the same process parameters. This proves that the active cooling method is more effective than traditional convection and radiation, which leads to quicker solidification of the liquid molten material and therefore smaller bead width. It is interesting to observe that the process window and the contour line in group III are more close to those in group I, which implies that the heat dissipation of the upper layer might reach the same level as that of the lower layer with the aid of active cooling. Figure 5 compares the molten pool shapes and the corresponding forming appearances obtained in groups II and III under the same parameters of WFS = 5.5 m/min and TS = 37 cm/min (at the high heat input region). Without cooling, the molten pool flows randomly with interactions of various forces and the edge has a tendency to collapse. The remelting of the substrate (previous layer) is also obvious as shown in Fig. 5a. This phenomenon disappears when active cooling is applied and the molten pool exhibits a cone shape. This proves that with active cooling it is possible to eliminate the impact of excessive heat input on the molten pool shape and ultimately the forming quality.

Further, how active cooling affects the microstructures of additively manufactured parts was investigated. The microstructures in the middle of the beads from Fig. 5 were characterized by dendrite grains, as shown in Fig. 6. The average grain size was 8.85 μm when active cooling was applied, compared to 16.53 μm obtained without active cooling. This is because active cooling generates a much larger heat dissipation rate that helps increase the number of particles and therefore refine the grain size.

3.2 Comparison of deposition rate in the three cases

This contour plot above gives an instruction about how to select appropriate WFS and TS to obtain the desired bead width. For a certain bead width, we can obtain different combination of WFS and TS. From the viewpoint of high efficiency, the WFS should be as high as possible because the deposition rate (DR) is determined by Eq. (1) as follows:

$$\mathrm{DR} = \frac{\rho \pi d^2}{4} \times \mathrm{WFS} \tag{1}$$

The maximum allowable WFS as well as the maximum DR without and with active cooling is obtained from Fig. 4, which

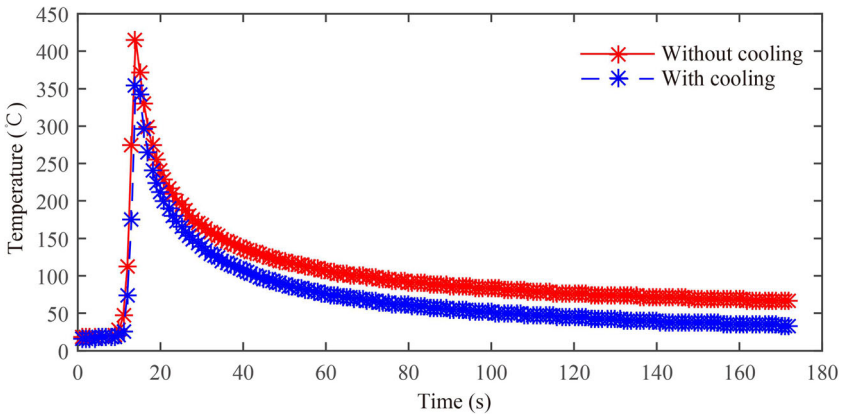

Fig. 7 Comparison of thermal cycling curves with and without cooling

Table 3 Inter-layer dwell time versus inter-layer temperature

Inter-layer temperature	50 °C	75 °C	100 °C
Cooling time without cooling	180 s	131 s	70 s
Cooling time with cooling	91 s	60 s	40 s
Reduction	− 50%	− 54%	− 42%

is a function of the bead width as summarized in Table 2. Active cooling allows enlarged process window and therefore more process parameters can be chosen for a certain bead width. The maximum deposition is improved by 9–15% for the bead width of 8–14 mm.

3.3 Comparison of inter-layer dwell time in the three cases

Heat accumulation is another factor that significantly affects the molten pool shape and the forming quality [25]. To avoid this, the inter-layer temperature should be well controlled through setting the appropriate inter-layer dwell time. Figure 7 compares the thermal cycling curves without and with cooling measured by thermocouples, from which we can obtain the peak temperature and the inter-layer dwell time as a function of the inter-layer temperature. With active cooling, the peak temperature is decreased obviously from 415 to 353 °C and the cooling rate is increased significantly. As a consequence, the inter-layer dwell time is decreased by 42–54% for the inter-layer temperature of 50–100 °C, as given in Table 3.

From the above analysis, we can conclude that active cooling has significant effect on the molten pool both before and after it is solidified. Therefore, it allows for increased efficiency through two ways. One is to increase the maximum deposition rate (9–15%) and the other is to decrease the inter-layer dwell time (42–54%).The overall improvement of the efficiency depends on the actual case.

3.4 Case study

To further verify the benefits of active cooling, three walls were fabricated with different process parameters, which were 100 mm long and were made of 10 layers, as given in Table 4. The inter-layer temperature was retained at room temperature. In order to build a wall of 10-mm width, the required

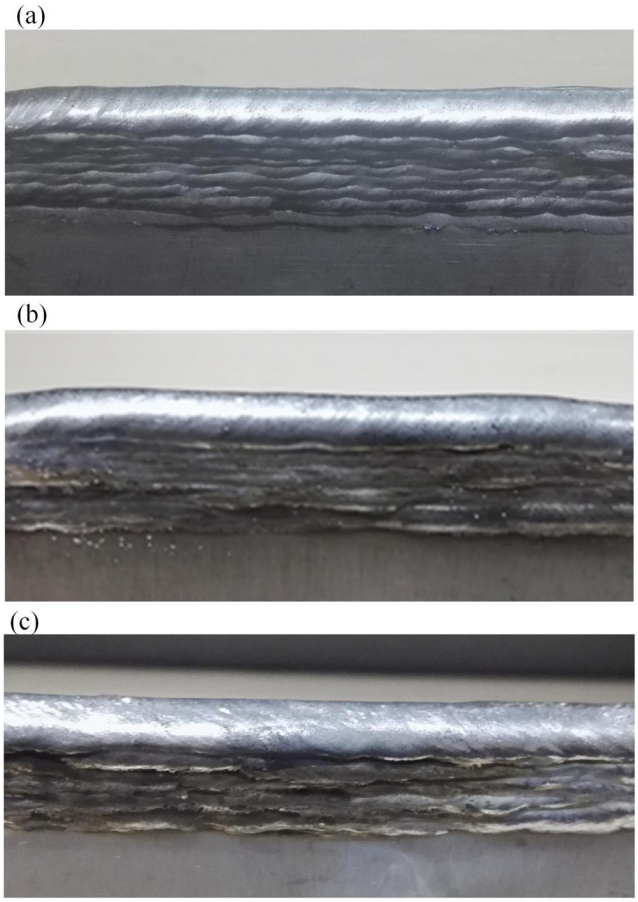

Fig. 8 Wall structures when: **a** WFS = 3 m/min and TS = 30 cm/min without cooling, **b** WFS = 5 m/min and TS = 50 cm/min with cooling, **c** WFS = 5 m/min and TS = 50 cm/min without cooling

WFS and TS were 3 m/min and 30 cm/min respectively without cooling (case a), which took 3.3 min in deposition time and 54 min in cooling time. If active cooling was applied, WFS and TS could be increased to 5 m/min and 50 cm/min respectively while maintaining the same bead width (case b), which took 2 min in deposition time and 27 min in cooling time. The decrease of the cooling time is more significant than that of the deposition time. The overall efficiency is improved by 0.97 times. The third case employed the same process parameters as the second case but the active cooling was not applied. The obtained bead width was about 12 mm and the required total time was 56 min, which means lower material utilization and lower efficiency compared with the case with cooling. The advantage of active cooling is clearly demonstrated (Fig. 8).

Table 4 Parameter settings and results in the case study

Case no.	WFS (m/min)	TS (cm/min)	Width (mm)	Height (mm)	Deposition time (min)	Cooling time (min)	Total time (min)	Cooling condition
a	3	30	10	22	3.3	54	57.3	Without
b	5	50	10	22	2	27	29	With
c	5	50	12	18	2	54	56	Without

4 Conclusions

This paper proposes an in-process active cooling technology to compensate for the excessive heat input associated with the high WFS during TG-WAAM. Its effect on forming quality and efficiency is investigated. The conclusions are as follows:

(1) The heat dissipation condition becomes worse with the increase of the deposition height, which confines the process window and is likely to cause molten pool overflowing.
(2) Thermoelectric technology–based active cooling contributes to enhancing the heat dissipation of upper layers that leads to larger process window and better control of the molten pool shape. The bead tends to be narrower and the average decrease is about 2 mm.
(3) With the assist of active cooling, the maximum WFS can be increased by 9–15% and the inter-layer dwell time can decreased by 42–54% while maintaining the desired forming quality.
(4) The case study shows that the overall efficiency is improved by more than 0.97 times when active cooling is applied attributed to both increased maximum WFS and decreased inter-layer dwell time.

Funding information This work was supported by the National Natural Science Foundation of China (no. 51805013) and Foundation Research Fund of Beijing University of Technology (no. 001000546318526).

Publisher's Note Springer Nature remains neutral with regard to jurisdictional claims in published maps and institutional affiliations.

References

1. Thompson MK, Moroni G, Vaneker T, Fadel G, Campbell RI, Gibson I, Bernard A, Schulz J, Graf P, Ahuja B, Martina F (2016) Design for additive manufacturing: trends, opportunities, considerations, and constraints. CIRP Ann Manuf Technol 65(2):737–760
2. Li F, Chen S, Wu Z, Yan Z (2018) Adaptive process control of wire and arc additive manufacturing for fabricating complex-shaped components. Int J Adv Manuf Technol 96(1–4):871–879
3. ZhongY RLE, Wikman S, Koptyug A, Liu L, Cui D, Shen ZJ (2017) Additive manufacturing of ITER first wall panel parts by two approaches: selective laser melting and electron beam melting. Fusion Eng Des 116:24–33
4. Martina F (2014) Investigation of methods to manipulate geometry, microstructure and mechanical properties in titanium large scale wire+arc additive manufacturing. Dissertation, Cranfield University
5. Baufeld B, Biest OVD, Gault R (2010) Additive manufacturing of Ti–6Al–4V components by shaped metal deposition: microstructure and mechanical properties. Mater Des 31(1):S106–S111
6. Xu X, Ding J, Ganguly S, Diao C, Williams S (2017) Oxide accumulation effects on wire + arc layer-by-layer additive manufacture process. J Mater Process Technol 252:739–750
7. Ding D, Pan Z, Cuiuri D, Li H (2015) Wire-feed additive manufacturing of metal components: technologies developments and future interests. Int J Adv Manuf Technol 81(1–4):465–481
8. Ding D, Pan Z, Cuiuri D, Li H (2015) A practical path planning methodology for wire and arc additive manufacturing of thin-walled structures. Robot CIM-INT Manuf 34(C):8–19
9. Zhan Q, Liang Y, Ding J, Williams S (2016) A wire deflection detection method based on image processing in wire + arc additive manufacturing. Int J Adv Manuf Technol 89(1–4):1–9
10. Li F, Chen S, Shi J, Zhao Y (2018) In-process control of distortion in wire and arc additive manufacturing based on a flexible multi-point support fixture. Sci Technol Weld Joi. https://doi.org/10.1080/13621718.2018.1476083
11. Li F, Chen S, Shi J, Tian H, Zhao Y (2017) Evaluation and optimization of a hybrid manufacturing process combining wire arc additive manufacturing with milling for the fabrication of stiffened panels. Appl Sci 7(12):1233
12. Xiong J, Lei Y, Chen H, Zhang G (2017) Fabrication of inclined thin-walled parts in multi-layer single-pass GMAW-based additive manufacturing with flat position deposition. J Mater Process Technol 240:397–403
13. Xiong J, Zhang G, Zhang W (2015) Forming appearance analysis in multi-layer single-pass GMAW-based additive manufacturing. Int J Adv Manuf Technol 80(9–12):1767–1776
14. Geng H, Li J, Xiong J, Lin X (2016) Optimisation of interpass temperature and heat input for wire and arc additive manufacturing 5A06 aluminium alloy. Sci Technol Weld Joi 22(6):472–483
15. Xiong J, Zhang G, Hu J, Wu L (2014) Bead geometry prediction for robotic gmaw-based rapid manufacturing through a neural network and a second-order regression analysis. J Intell Manuf 25(1):157–163
16. Xiong J, Yin Z, Zhang W (2016) Closed-loop control of variable layer width for thin-walled parts in wire and arc additive manufacturing. J Mater Process Technol 233:100–106
17. Ye D, Hua X, Wu Y (2013, 2013) Arc interference behavior during twin wire gas metal arc welding process. Adv Mater Sci Eng: 937094
18. Sproesser G, Chang YJ, Pittner A, Finkbeiner M, Rethmeier M (2017) Environmental energy efficiency of single wire and tandem gas metal arc welding. Weld World 61(4):733–743
19. Li F, Chen S, Shi J, Zhao Y, Tian H (2018) Thermoelectric cooling-aided bead geometry regulation in wire and arc-based additive manufacturing of thin-walled structures. Appl Sci 8(2):207
20. Ding J (2012) Thermo-mechanical analysis of wire and arc additive manufacturing process. Dissertation, Cranfield University
21. Henckell P, Günther K, Ali Y, Bergmann JP, Scholz J, Forêt P (2017) The influence of gas cooling in context of wire arc additive manufacturing—a novel strategy of affecting grain structure and size. TMS 2017 146th Annual Meeting & Exhibition Supplemental Proceedings. Springer International Publishing
22. Cong B, Qi Z, Qi B, Sun H, Zhao G, Ding J (2017) A comparative study of additively manufactured thin wall and block structure with al-6.3%cu alloy using cold metal transfer process. Appl Sci 7(3):275
23. Meng JH, Wang XD, Zhang XX (2013) Transient modeling and dynamic characteristics of thermoelectric cooler. Appl Energy 108(5):340–348
24. Zhao D, Tan G (2014) A review of thermoelectric cooling: materials modeling and applications. Appl Therm Eng 66(1–2):15–24
25. Wu B, Ding D, Pan Z, Cuiuri D, Li H, Han J, Fei ZY (2017) Effects of heat accumulation on the arc characteristics and metal transfer behavior in wire arc additive manufacturing of Ti6Al4V. J Mater Process Technol 250:304–312